Dynamic Behavior of a Pure Fluid at and around its Critical Density under microgravity and 1g [1]

C. Bartscher[2] and J. Straub[2,3]

[1] Paper presented at the Fourteenth Symposium on Thermophysical Properties, June 25-30, 2000, Boulder, Colorado, U.S.A.

[2] Technische Universitaet Muenchen, Lehrstuhl A fuer Thermodynamik, Boltzmannstrasse 15, D-85748 Garching, Germany

[3] To whom correspondence should be addressed

ABSTRACT

A new sample cell allowing accurately measurable density quenches was developed for a further investigation of the dynamic temperature propagation or piston effect. Several experiments were performed under 1g and µg during the Perseus mission in 1999. For the 1g experiments the starting temperatures relative to Tc ranged in the one phase region between 100 and 1000 mK and under µg between 50 and 100 mK, respectively, while the density varied between $0.7\ \rho_C < \rho < 1.3\ \rho_C$. The difference between 1g and µg for the temperature relaxation is shown and the isentropic difference coefficients $(\Delta\rho/\Delta T)_S$ and $(\Delta T/\Delta P)_S$ are determined and compared with the equation of state for SF_6.

KEY WORDS: piston effect; dynamic temperature propagation; SF_6; Perseus mission; Alice 2 Facility; microgravity; isentropic coefficients

1 INTRODUCTION

A sudden rise in temperature in the wall of a sample cell with a finite volume causes a thermal expansion of the fluid in the boundary layer resulting in a compression of the bulk fluid with an average pressure and temperature increase. This effect is known as the "piston effect" or dynamic temperature propagation. Assuming negligible temperature gradients outside the boundary layer, the compression is adiabatic. In addition, using the assumption that no energy is dissipating, the compression is isentropic. Thus there will be a temperature increase [1-3] in the bulk. Therefore the energy transport to the center of the cell is a mechanical process, propagating like a pressure wave defined by the speed of sound w_s and the isentropic compressibility χ_s [4]. The thermal propagating process is not caused by thermal diffusivity only as had been assumed for a long time. Such diffusion would result in long thermal relaxation processes since the thermal diffusion approaches zero near the critical point.

While Eicher [1] heated the surface of a cell some piston effect experiments were performed using a thermistor in the cell's fluid as a heater, e.g. [5]. However, a large power input for several seconds was necessary due to the small heater surface before measurable results could be achieved. Since many analytical approaches favor a step like temperature change we used a different method performing rapid ($t<0.4$ seconds) density quenches at a constant wall temperature as the boundary condition. Measuring temperature and pressure changes in the fluid (ΔT, ΔP) fast enough and with high resolution the difference coefficients can be regarded as differential coefficients when the step size of $\Delta\rho$ is small.

Several isentropic coefficients $\left(\frac{\partial P}{\partial \rho}\right)_S$, $\left(\frac{\partial T}{\partial \rho}\right)_S$ or $\left(\frac{\partial P}{\partial T}\right)_S$ can be calculated and from the temperature and average density change the isentropic expansion coefficient α_s be determined with

$$a_s = -\frac{1}{\rho}\left(\frac{\partial \rho}{\partial T}\right)_s, \text{ with } \left(\frac{\partial \rho}{\partial T}\right)_S \sim \left.\frac{\Delta \rho}{\Delta T}\right|_S . \qquad (1)$$

as well as the isentropic compressibility χ_s from the related average change in pressure Δp

$$c_S = \frac{1}{\rho}\left(\frac{\partial \rho}{\partial P}\right)_S, \text{ with } \left(\frac{\partial \rho}{\partial P}\right)_S \sim \left.\frac{\Delta \rho}{\Delta P}\right|_S \qquad (2)$$

and with Δp and ΔT the isentropic tension coefficient β_s

$$b_S = \frac{1}{P}\left(\frac{\partial P}{\partial T}\right)_S, \text{ with } \left(\frac{\partial P}{\partial T}\right)_S \sim \left.\frac{\Delta P}{\Delta T}\right|_S \qquad (3)$$

With these isentropic coefficients further thermodynamic relations can be derived, such as the speed of sound or the isochoric specific heat capacity

$$w_S = \rho c_S^{-\frac{1}{2}} \text{ and } c_V = -\frac{\rho}{PT} a_S b_V \quad \text{with} \quad b_V = \frac{1}{P}\left(\frac{\partial P}{\partial T}\right)_V, \qquad (4)$$

and used as a check for the consistency of thermodynamic equations, especially in the near critical region where several thermodynamic properties diverge.

2 EXPERIMENTAL SETUP

In order to perform accurate density quenches and measure the corresponding dynamic pressure and temperature response we developed a sample cell (Fig. 1) that was divided into a compensation (storage) and an observable measurement volume. In the 12 mm diameter compensation volume a piston could be moved backward and forward in

small (0.5% $\rho_C < \Delta\rho < 1.5\% \rho_C$) but rapid steps. The maximum possible translation of the piston was 15 mm allowing for a maximum ±40% density change. The measurement volume had a diameter and height of 12 mm each, with sapphire windows at both ends giving the cell a cylindrical shape.

An ENTRAN piezoelectric-resistive pressure sensor was installed as well as three USER thermistors (Thermometrics B10KA103K). Each bead was 0.25 mm in diameter including its glass coating with a thermal time constant of 10 msec. One thermistor T_1 was installed within 0.5 mm of the center of the cell, the second thermistor T_2 was positioned 0.67 mm off the aluminum wall inside the fluid, while a third thermistor T_3 was mounted into the wall within 1 mm to the fluid to measure the effect of the changing fluid temperature on the wall of the cell after the density quenches.

The two volumes were interconnected through a canal of 1 mm in diameter which was leading through a ball valve. During the piston effect (PE) experiments or when the fluid's average density was brought to the next desired setting the valve was in the open position. After a sufficient long waiting period during which the density in the fluid cell had been homogenizing at temperatures far above the critical temperature, typically T_c + 2 K, the valve was closed so that the cell could also be used for phase separation experiments. The valve was necessary mainly for two reasons. Since only the measurement volume could be observed by video, and in order to prevent it from being influenced by effects occurring unseen inside the compensation volume, both must be separated from each other. Furthermore, by closing the valve after each density setting, the shape and the volume to surface ratio of the measurement volume remained unchanged. This left the

density as the only variable which simplified the comparison of the phase separation and the PE experiments.

The fluid cell with its two volumes, the piston and its mechanism, and the valve and its mechanism were mounted into an aluminum cylinder (60 mm in diameter, 115 mm in height) known as the sample cell unit (SCU). Three additional thermistors are spread over the SCU functioning as measurement, control and over-heat sensors for the facility's temperature control. The SCU was inserted into a three-shield thermostat by the Van-der-Waals-Zeeman laboratory at the University of Amsterdam (Fig.2). It was equipped with a number of heater foils, thermistors, Peltier elements, and thermocouples for temperature control.

For μg measurements on MIR the thermostat was inserted in the Aerospatiale-built and CNES-funded Alice-2 facility which provided a very stable temperature environment (40 μK/h) with relative resolution of 100 μK [6]. The temperature and pressure data was collected at a rate of 25 Hz during PE measurements, while live video images of the fluid cell were recorded on video tape. The thermostat was modified such that during experiment operation the valve and the piston can be operated from the outside. After proper calibration a scale and a counter helped defining the accurate density settings and determination of the density quenches within ±0.03% ρ_c. During phase separation experiments the piston mechanism could be disconnected from the SCU to minimize thermal leaks.

This unique construction of fluid cell and thermostat and the capabilities of Alice-2 gave independent control of T and ρ, the two appropriate variables for the systematic

determination of the piston effect. The average starting density of the fluid could be varied in a range of 0.7 $\rho_c > \rho > 1.35\ \rho_c$ with a resolution of 0.2 % with respect to ρ_c while most starting temperatures used were in a range of $-100\ mK < T-T_C < +100\ mK$. Unfortunately it was not possible to implement a stepping motor for the piston movements as the experiments were suggested after Alice 2 had been built and transported to MIR and there was no interface available for the necessary power supply and coordinated control possibilities. Therefore all mechanical movements were performed with a special tool by hand of the cosmonaut. This leads naturally to a wider spectrum in terms of quench time, but varies mostly in a small range of $0.28\ sec < t < 0.41\ sec$.

In the case of 1g experiments a laboratory setup was used with a temperature control identical to the Alice facility and therefore similar control stability. The main difference was in the data acquisition by using a Keithley 2001 multi-scanner. It allowed only a 10 Hz measurement frequency per sensor, however, the noise level of 3.8 mbar rms with an adequate filter and a resolution of 2 mbar (lsb) of the pressure sensor data was about 10 times better than with the facility. The temperature resolution of 0.6 mK with a noise level of 0.4 mK rms was similar in both cases.

3 EXPERIMENTAL RESULTS

A series of PE experiments was performed under 1g and microgravity with SF_6 (T_C = 318.717 K, P_C = 3.7545 MPa, $\rho_C = 742\ kg \cdot m^{-3}$, [7]) as the test fluid. First a temperature was set typically 2 K above the critical temperature for homogenization, then the fluid was cooled down slowly to the desired starting temperature. With the valve open the fluid was given sufficient time for reaching a homogeneous temperature and density state. The

subsequent density quench was performed in a rapid and uniform way, typically with a quench time of t_{quench} = 350 msec ± 100 msec and a size of the quench of $\Delta\rho_{quench}$ = 0.0088 ρ_C ±5%. The procedure was identical for each experiment both 1g and µg. The starting temperatures at which a density quench was performed were $T - T_C$ = 10, 50, 100, 200, 500 and 1000 mK for 1g and $T - T_C$ = 30, 50, and 100 mK for µg, with an average starting density ranging $0.7\ \rho_C < \rho < 1.35\ \rho_C$.

In a first step we compare our measurements with an analytical approach for various boundary conditions as derived by [1], here only for the case of a stepwise temperature change in the wall [2].

$$\frac{T_W - T(x,t)}{T_W - T_i} = \exp\left(-2\frac{\sqrt{t}}{\sqrt{t_{char}}}\right) \bullet erfc\left(\frac{x}{2\sqrt{Dt}}\right) \qquad (5)$$

T(x,t) is the actual temperature in the fluid and D the thermal diffusivity. Although our initial conditions were different with a constant wall temperature and a temperature rise in the fluid due to the density quench, this approach is still useful for a preliminary check. Furthermore, one can fit the experiment conditions to the demands of the analytical approach by regarding the peak temperature after the quench as the whole system's initial temperature $T_0(t=0) = T_i$ and the wall temperature T_W as the result of a fictitious negative temperature step ($\Delta T = T_W - T_i$). T_W is regarded as constant thereafter. The characteristic time t_{char} is defined as

$$t_{char} = \left[\left(\frac{c_p}{c_v} - 1\right)\sqrt{D}\,\frac{A}{V}\,\frac{2}{\sqrt{p}}\right]^{-2} \qquad (6)$$

The influence of the system geometry is defined by the surface area (A) to Volume (V) ratio, where A is the area of the heated or cooled surface. A can therefore be regarded as the “piston area”. With increasing A/V ratio the characteristic time t_{char} decreases and the temperature change in the bulk is accelerated. In our case the size of diameter and height of the cylindrical shape is identical, therefore the A/V ratio equals to 3/R with R as the radius. Since this is also true for a spherical cell we regard our cell as such and simplify the problem to a 1-dim. one. In Table I the characteristic time t_{char} for SF_6 is given as a function of $T - T_C$ for the critical and one far super- and subcritical density according to Eq. (6) for the position of the center thermistor T_1 (x = 5.54 mm). For simplicity it is assumed that the fluid properties are constant. The thermal diffusivity D is calculated after Jany [8] and Kruppa [9], and the specific heat capacities c_p and c_v with Wyczalkowska and Sengers’ equation of state [10]. According to [2] Eq. (5) is valid only under the assumption that

$$t << t_{char}.$$

With the numbers in Table I it is obvious that the validity of Eq. (5) is very limited, especially for critical and near critical densities. For the far off critical densities the problem is less crucial due to the longer times.

This is confirmed by the following series of 1g and µg measurements performed at $T_W = T_C + 100$ mK for various densities. The 1g and µg curves show the temperature homogenization at x = 5.54 mm (center thermistor) after a density quench in a range of $0.75\ \% \rho_C < \Delta\rho < 8.8\% \rho_C$. In Fig. 3a the dynamic temperature propagation is plotted for the critical density $\rho = \rho_C$. While the analytical approach shows quick temperature equalization that is 99% finished in less than 1 second, for 1g and µg a much longer time is

required. In Figs. 3 b to d the results are plotted for $\rho = 1.1\ \rho_C$, $\rho = 1.2\ \rho_C$, and $\rho = 1.3\ \rho_C$, respectively. In all cases the analytical approach is much faster than in the experiments which confirms that Eq. (5) has an only limited validity, but can be used very well for estimating the influence of the fluid properties, the geometry and the tendency of the system on the speed of the temperature equilibration for short times. However, the further away the density is from the critical density the better the agreement between the analytical and the 1g plots. Also the difference to the µg plots shrinks remarkably. The difference between the 1g and µg temperature equilibration shows the influence of the convection versus the homogenization from the pure piston effect under µg. It shows that although the piston effect is dominant in both regimes convection can not be neglected even within the first few seconds after the density quench.

Fig. 4 presents the isentropic difference coefficients $(\Delta\rho/\Delta T)_s$ for various 1g and µg experiments at three different temperatures ($T-T_C$ = 1000 mK, 100 mK, 50 mK) in comparison with the Senger's equation of state [10]. As it was possible to perform far more PE experiments under 1g the results for T_C +1000 mK and +100 mK are given as a mean value with a bar showing the range of values from various experiments at distinct densities. It is obvious that all experimental values exceed the theoretical values by 6% to 27 %, with the larger deviation in the near critical density region. While the size of the density change $\Delta\rho$ can be accurately calculated within ±2%, the larger uncertainty is with the determination of ΔT for mainly two reasons.

Since we tried to keep the quench time as short as possible (typically 250 to 450 msec) the frequency of data acquisition was only about 10 Hz per channel therefore the

temperature difference between two data point could easily be 40 mK or more. Hence it is very unlikely that the highest temperature point acquired was really the largest value that should be reached due to the quench. The other point that may contribute to the error even more is the piston effect itself. Although the quenches were performed quickly the piston effect is initiated as soon as the temperatures of fluid and wall are different. In addition convection sets in, counteracting the temperature rise together with the piston effect as soon as the quench is started. This also prevents the fluid from reaching its theoretical temperature peak leading to a smaller ΔT. Preliminary estimations show that the size of both effects would be in the order of magnitude explaining the difference between theory and measurement values. A correction would therefore increase ΔT leading to more correct coefficient values.

Consistent with the above findings are the results from the μg measurements performed during the French-Russian Perseus mission in summer 1999 on board the MIR space station. Especially the results from the PE runs performed at T_C +50 mK show relatively good agreement with theory for both the sub- and supercritical density region. The reason that those points fit even better than the 1g point probably lies in the absence of convection which has a significant contribution to the speed of temperature relaxation as can be seen in Fig. 3. However, the reason why some of the T_C +100 mK points deviate more is not fully understood yet.

In Fig. 5 the critical and supercritical density results are plotted for the isentropic difference coefficient $(\Delta T/\Delta P)_S$ for the temperature range of 1 mK < $T-T_C$ < 1 K in comparison with the theoretical solutions of the equation of state [10]. Only 1g data are

available since the noise level of the µg pressure data was unacceptably high not allowing reasonable calculations. The 1g data, however, are in relatively good agreement with the theoretical data when the ΔT correction for piston effect and measurement error is taken into consideration again.

4 CONCLUSION

Preliminary results show that both 1g and µg data are in reasonable agreement with the calculated values from the equation of state. However it must be considered, that the piston effect starts cooling down the bulk as soon as the quench is initiated. Therefore the peak value of temperature could not be reached. Also the measurement method with its still too slow acquisition rate compared with rapid temperature change during the quench has to be taken into consideration and the values should be corrected for these effects. Still this method of using density quenches, which can be performed magnitudes faster than a temperature quench, offers a good technique to determine the isentropic coefficients $(\Delta\rho/\Delta T)_S$ and $(\Delta T/\Delta P)_S$. The comparison of 1g and µg temperature relaxation data shows that the piston effect is dominant in both cases and that convection can not be neglected even within the first few seconds after the density quench.

ACKNOWLEDGEMENTS

This research was supported by Deutsches Zentrum für Luft- und Raumfahrt e.V. (DLR) under grant number 50WM9604. The above-described German µg experiments were performed on the MIR space station as part of the French MIR mission PERSEUS made possible under a French-German co-operation contract between CNES and DLR. We

would like to thank B. Zappoli and J.-F. Zwilling from the French space agency CNES, Toulouse and Y. Garrabos and C. Chabot from ICMCB, Bordeaux for their support and fruitful discussions. We are also grateful to the Van-der-Waals-Zeeman laboratory of the University of Amsterdam for building our thermostats and are indebted to J.V. Sengers for leaving us a copy of his equation of state for SF_6.

REFERENCES

1 J. Straub, L. Eicher, and A. Haupt, Phys. Rev. E, Vol. 51, No. 6, 5556 (1995)

2 A. Onuki, H. Hao, and R. A. Ferrell, Phys. Rev. A. Vol. 41, 2256 (1990)

3 A. Onuki and R.A. Ferrell, Physica A 164, 245 (1990)

4 H. Boukari, J. Shaumeyer, M. Briggs, and R. Gammon, Phys. Rev. A, Vol.41, (1990)

5 T. Fröhlich, P. Guenoun, M. Bonetti, F. Perrot, D. Beysens, Y. Garrabos, B. Le Neindre, and P. Bravais, Phys. Rev. E, Vol. 54, No. 2, 1544 (1996)

6 R. Marcout, J.-F. Zwilling, J. M. Laherrere, Y. Garrabos, D. Beysens, *ALICE 2, an advanced facility for the analysis of fluids close to their critical point in microgravity*, presented at 45th Congress of the International Astronautical Federation, Jerusalem, Israel, 1994

7 W. Wagner, N. Kurzeja, and B. Pieperbeck, Fluid Phase Equilibria **79**, 151 (1992)

8 P. Jany, Ph.D. Thesis, Technische Universität München, (1986)

9 B. Kruppa, Ph.D. Thesis, Technische Universität München, (1993)

10 A. K. Wyczalkowska and J. V. Sengers, Journal of Chem, Phys., Vol. 111, No. 4, 1551 (1999)

TABLES

Table I: Characteristic time t_{char} after Eq. (6) as a function of temperature and density

$T-T_C$, mK	10	50	100	200	500	1000
t_{char} ($\rho=\rho_C$), s	0.0009	0.01	0.026	0.07	0.26	0.7
t_{char} ($\rho=1.3\ \rho_C$), s	24.1	17.7	16.1	15	14.8	16.0
t_{char} ($\rho=0.7\ \rho_C$), s	14.5	10.7	9.7	9.1	9.0	9.8

FIGURE CAPTIONS

Fig. 1. Fluid cell, valve and piston mechanism

Fig. 2. Aluminum fluid cell and sample cell unit (SCU) integrated in the three shell thermostat unit (THU).

Fig. 3. Dynamic temperature propagation in SF_6 during the first ten seconds after density quench. Analytical calculation with Eq. (5) versus 1g and µg measurements. Starting temperature before quench for all cases: $T-T_C = 100$ mK 1a) density $\rho = \rho_C$, 1b) $\rho = 1.1\ \rho_C$, 1c) $\rho = 1.2\ \rho_C$, 1d) $\rho = 1.3\ \rho_C$.

Fig. 4. Isentropic difference coefficient $(\Delta\rho/\Delta T)_S$ for various densities and temperatures under 1g and µg in comparison with equation of state [10].

Fig. 5. Isentropic difference coefficients $(\Delta T/\Delta P)_S$ for supercritical temperatures and densities in the range of $\rho_C < \rho < 1.3\ \rho_C$ under 1g in comparison with equation of state [10]

Figure 1

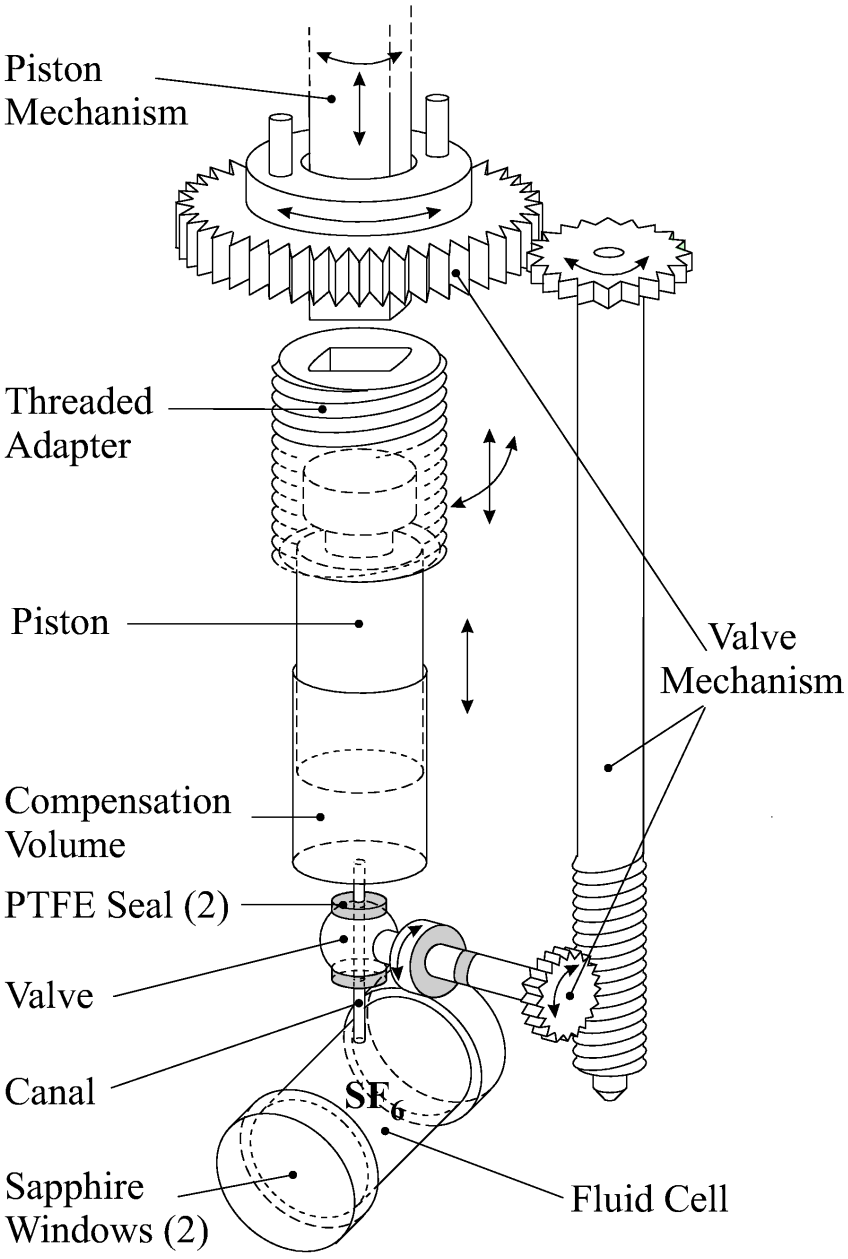
Piston
Mechanism
Threaded
Adapter
Piston
Valve
Mechanism
Compensation
Volume
PTFE Seal (2)
Valve
Canal
SF6
Sapphire
Windows (2)
Fluid Cell

Figure 2

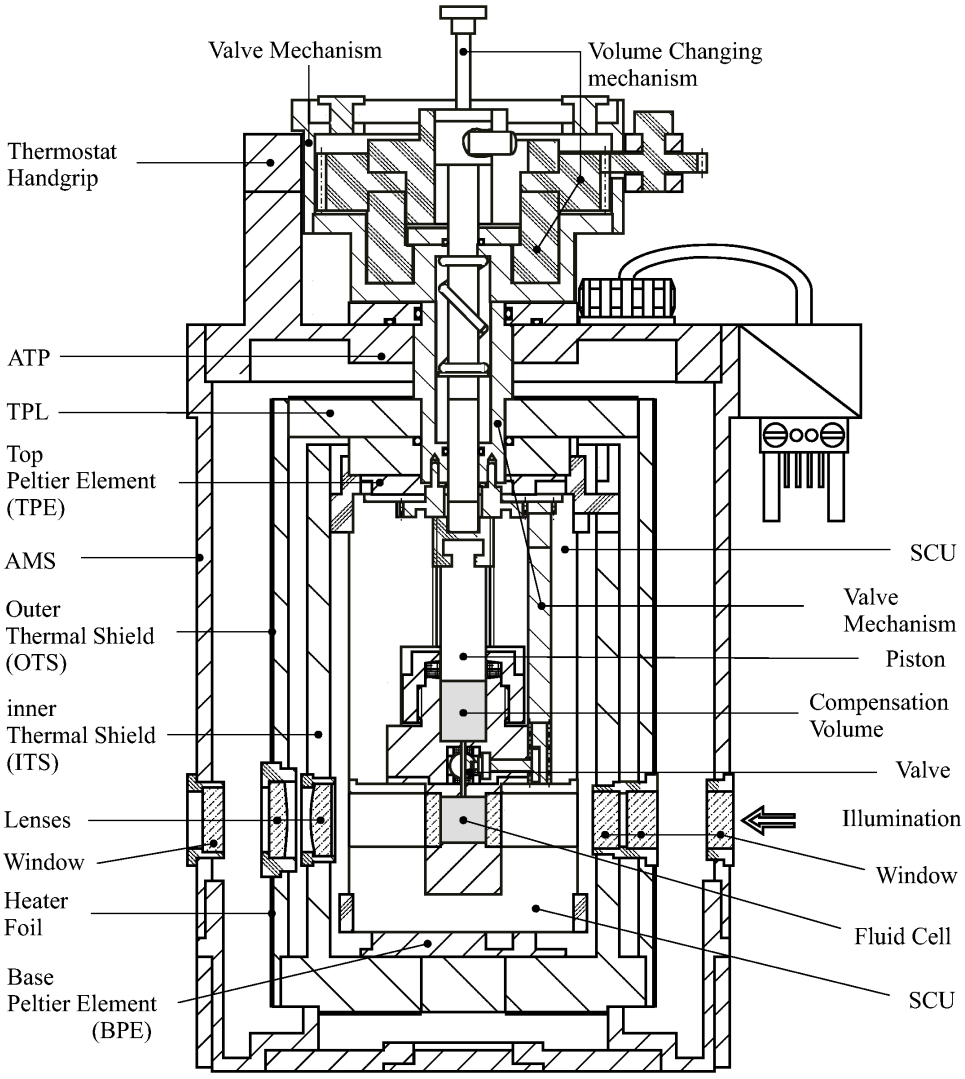
Valve Mechanism
Volume Changing mechanism
Thermostat Handgrip
ATP
TPL
Top Peltier Element (TPE)
AMS
Outer Thermal Shield (OTS)
inner Thermal Shield (ITS)
Lenses
Window
Heater Foil
Base Peltier Element (BPE)
SCU
Valve Mechanism
Piston
Compensation Volume
Valve
Illumination
Window
Fluid Cell
SCU

Figure 3

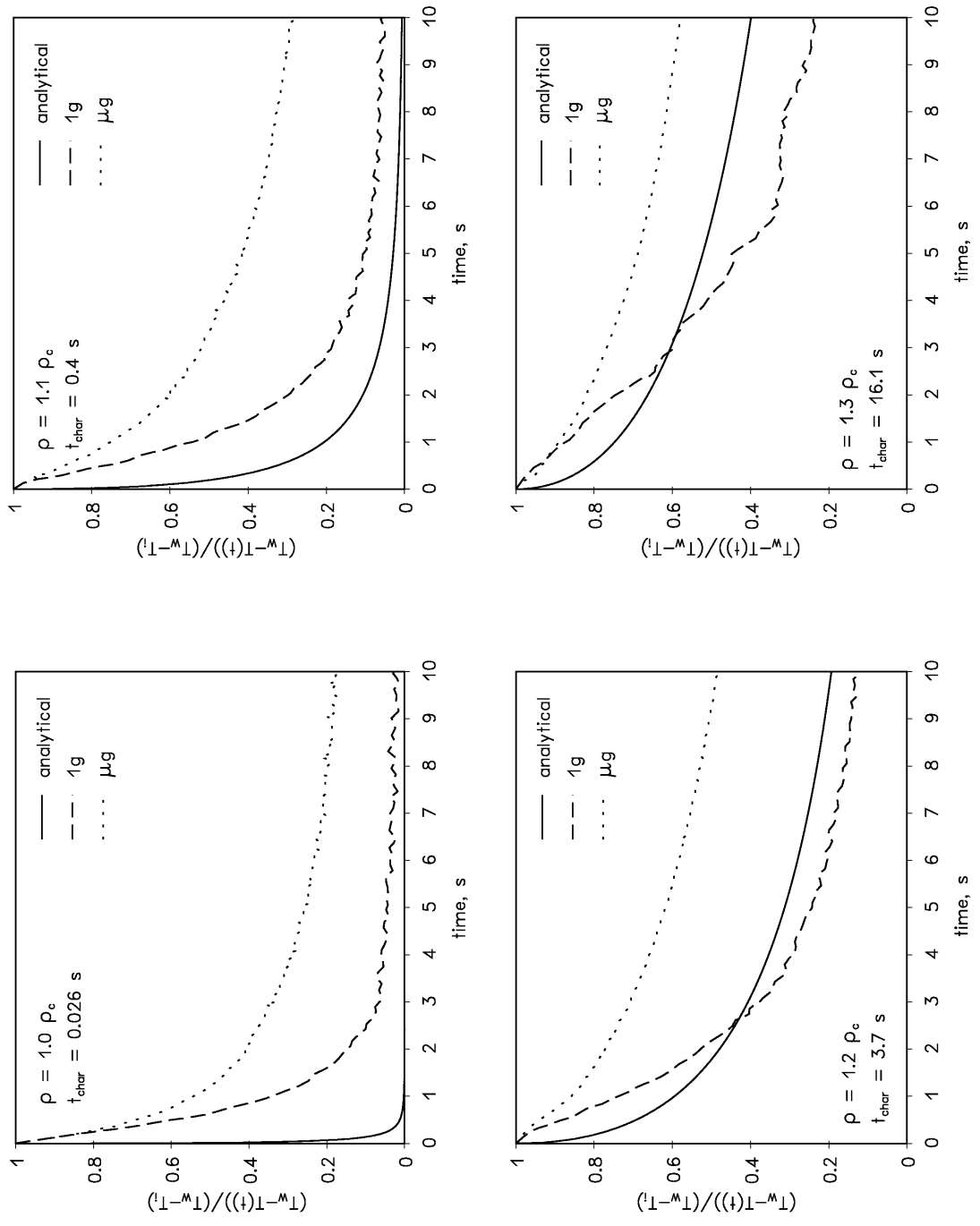
ρ = 1.0 ρc
tchar = 0.026 s
ρ = 1.1 ρc
tchar = 0.4 s
ρ = 1.2 ρc
tchar = 3.7 s
ρ = 1.3 ρc
tchar = 16.1 s
analytical
1g
μg
(Tw−T(t))/(Tw−Ti)
time, s

Figure 4

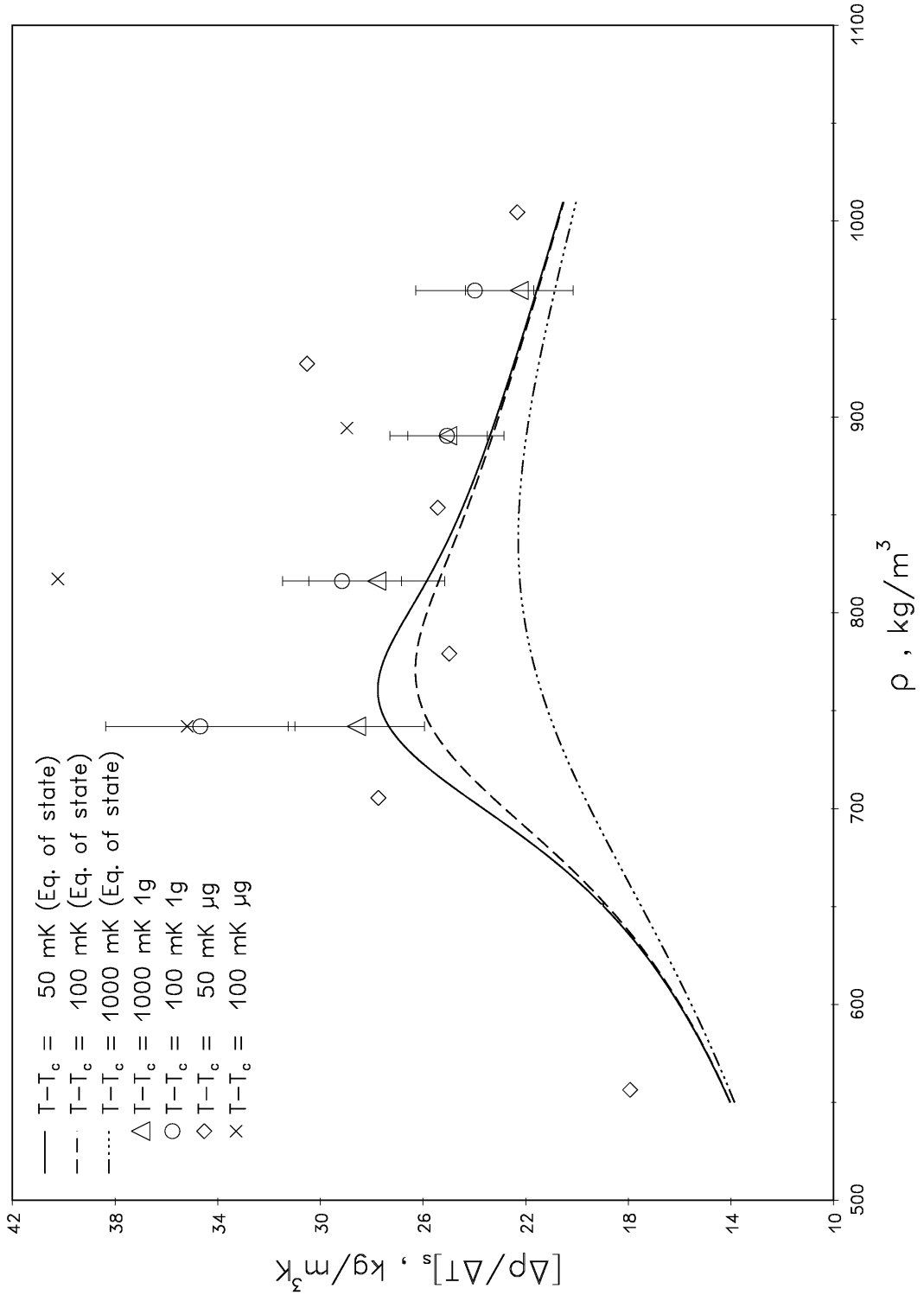
T−Tc = 50 mK (Eq. of state)
T−Tc = 100 mK (Eq. of state)
T−Tc = 1000 mK (Eq. of state)
T−Tc = 1000 mK 1g
T−Tc = 100 mK 1g
T−Tc = 50 mK μg
T−Tc = 100 mK μg
[Δρ/ΔT]s , kg/m3K
ρ , kg/m3
42
38
34
30
26
22
18
14
10
500
600
700
800
900
1000
1100

Figure 5

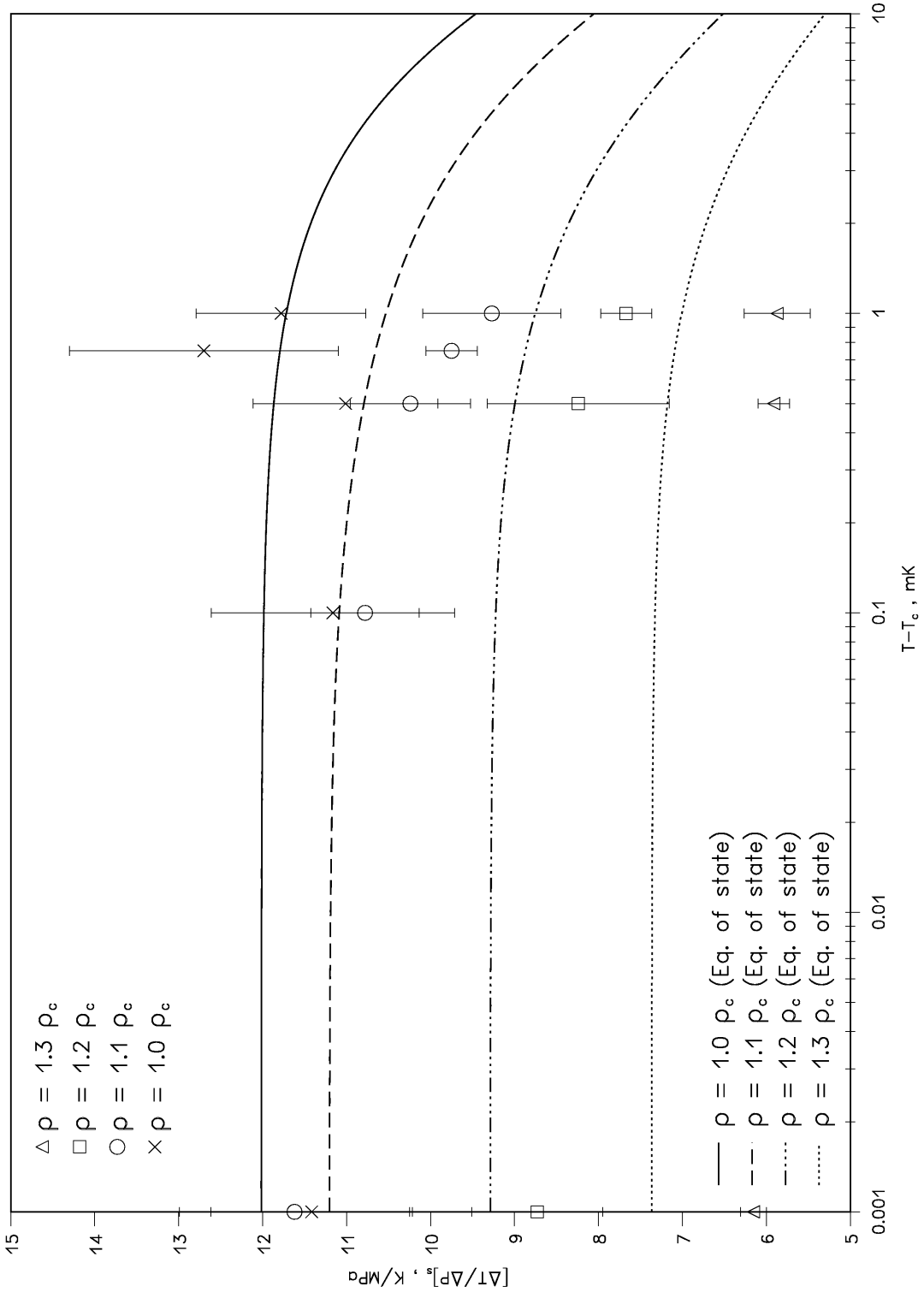
[ΔT/ΔP]s , K/MPa
T−Tc , mK
ρ = 1.0 ρc (Eq. of state)
ρ = 1.1 ρc (Eq. of state)
ρ = 1.2 ρc (Eq. of state)
ρ = 1.3 ρc (Eq. of state)
△ ρ = 1.3 ρc
□ ρ = 1.2 ρc
○ ρ = 1.1 ρc
× ρ = 1.0 ρc